16th Australasian Fluid Mechanics Conference
Crown Plaza, Gold Coast, Australia
2-7 December 2007

Characteristics of flow regimes for two plates of rectangular cross-section in tandem

A.M. Blazewicz[1], M.K. Bull[1] and R.M. Kelso[1]

[1]School of Mechanical Engineering
University of Adelaide, Adelaide, South Australia, 5005 AUSTRALIA

Abstract

Flow characteristics including velocity fluctuations, acoustic pressure fluctuations and surface pressures have been investigated for two plates in a tandem array at high Reynolds numbers. The plates were of rectangular cross section and of the same thickness, having and a range of chord-to-thickness ratios with a range of gap-to-thickness ratios between them. The flow measurements were complemented with hydrogen-bubble flow visualisation. A classification of possible flow regimes is proposed and confirmed experimentally. For very small separations the two plates behave as a single plate. Symmetrical vortex shedding is detected even for the configurations with larger separation. For the upstream plates in the single plate regime, where frequency components lower than the characteristic shedding frequency are present, these components are amplified in the presence of a downstream plate. They are clearly detectable in velocity and pressure measurements and can become dominant in the acoustic spectra.

Introduction

This research was conducted as a part of a general investigation of the regimes of fluid flow over bluff bodies in isolation and in tandem, and the radiation thereby produced. Flows such as these are a major cause of sound generation in turbomachinery, circular saws and other engineering equipment. This project is a basic study of these flow processes and the acoustic radiation they produce, using simplified representative models consisting of plates and plate arrays.

The results presented in this paper relate to tandem arrays of two plates P1 (upstream) and P2 (downstream) of the same thickness t and of rectangular cross-section, with chords c_1 and c_2 and a streamwise gap g between them. The geometry of the array is defined by the ratios $C_1 = c_1/t$, $C_2 = c_2/t$, and $G = g/t$. A dominant feature of the flow over such an array is flow separation from the leading edges of the upstream plate. The separated shear layers may impinge on the array further downstream or on each other downstream of the second plate, at a distance s (the impingement length) from the separation point. The point of impingement is not stationary; the non-dimensional impingement length $S = s/t$ will fluctuate between upper and lower limits S_{max} and S_{min}, over the range $\Delta S = (S_{max} - S_{min})$. Values of S will in general be similar to those for the leading-edge-separation bubble on a long single plate of rectangular cross-section, typically $S \approx 5 \pm 2$.

A proposed classification of flow regimes has been made by Bull, Blazewicz and Pickles [2] on the basis of the relative values of C_1, C_2, G, S_{min} and S_{max}. The ten possible regimes A to F3 are illustrated in figure 1. Some of the regimes have been investigated experimentally by Blazewicz and Bull [1]. Here, the results of the experimental investigation are expanded with the focus being on the flow patterns of the regimes. Three groups of arrays will be considered: **Group 1** with $C_1 < S_{min}$, **Group 2** with $S_{min} < C_1 < S_{max}$ and **Group 3** with $C_1 > S_{max}$.

Experimental Arrangements

All measurements were conducted at $3.2 \times 10^3 \leq Re_t\ (= Ut/\nu) \leq 53 \times 10^3$ with the plate arrays mounted between large end-plates so that the flow over them was nominally two-dimensional. Velocity fluctuations, and mean surface pressures were measured in an open-jet low-speed wind-tunnel using a hot-wire anemometer and surface static-pressure tappings respectively. Acoustic measurements were made in a separate facility located in a reverberation chamber. The plate arrays were subjected to the jet flow from a two-dimensional nozzle of the same width as the plates, fed from a compressed-air reservoir. Measurements were made while the pressure in the reservoir was allowed to run down continuously, giving a jet velocity slowly decreasing from about 200 m/s to about 15 m/s. Sound pressure levels were obtained as spatial averages from a condenser microphone traversing the reverberation chamber. Hydrogen-bubble flow visualisation experiments were performed in a water tunnel (maximum Reynolds number $Re_t \approx 3 \times 10^3$).

For a given plate configuration the differences in the Reynolds number between the water and air flows, leading to differences in the laminar-turbulent transition in the separated shear layers, in most cases, did not significantly affect the flow pattern. However the range of G at which a particular flow regime occurred was affected to some extend - as Reynolds number is increased the size of gap characterising the onset of any particular flow regime decreases. It was therefore assumed that flow patterns at high Reynolds numbers, at which flow and acoustic measurements were conducted, are generally similar to those obtained in the flow visualisation.

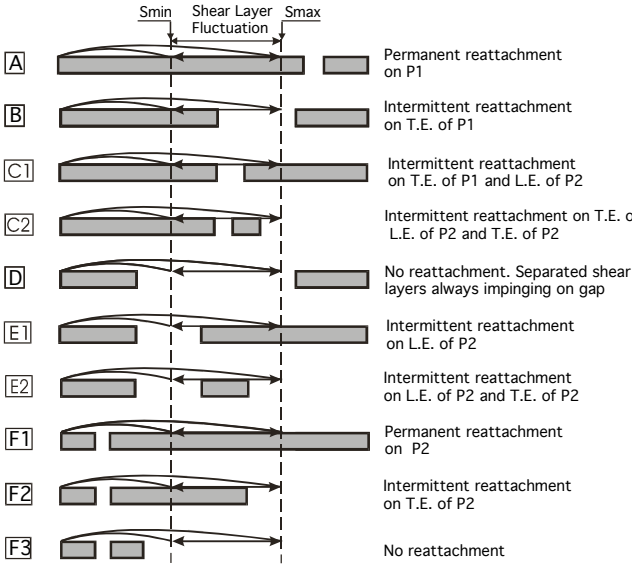

Figure 1. Schematic representation of possible flow regimes according to the plate configuration in relation to impingement length. L.E. refers to leading edge and T.E. to trailing edge.

GROUP 1: plate configurations with $C_1 < S_{min}$

In the investigation of the (C_1 = 1, C_2 = 1) array, flow visualisation shows that, for Reynolds number range covered, the regime F3 (which can also occur on a short single plate) persists only for gaps up to $G \leq 0.1$ (figure 2a). This regime is characterised by flow separation from the leading edges of plate P1, no reattachment, and von Karman vortex street formation downstream of plate P2. A symmetric mode can appear occasionally for a few shedding cycles as shown in figure 2b.
At $G = 0.3$ regime F2 starts to appear (figure 2c) with the shear layers separating from the leading edges of P1 and then reattaching periodically and intermittently to the streamwise surfaces of P2. Reattachment alternates from one side of P2 to the other, and there is flow through the gap, the direction of which reverses periodically.

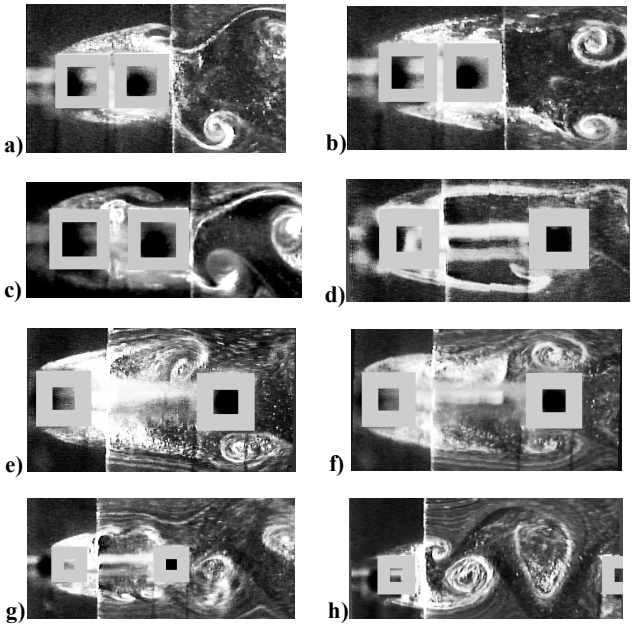

Figure 2. Flow over ($C_1 = C_2 = 1$) array: (a) $G = 0.1$, $Re_t \approx 1300$, asymmetric mode, (b) $G = 0.1$, $Re_t \approx 1300$, symmetric mode, (c) $G = 0.3$, $Re_t \approx 1300$, (d) $G = 1.5$, $Re_t \approx 600$, (e) $G = 2$, $Re_t \approx 1300$, asymmetric mode, (f) $G = 2$, $Re_t \approx 1300$, symmetric mode, (g) $G = 2$, $Re_t \approx 1900$, and (h) $G = 5$, $Re_t \approx 1300$.

In regime E2 (figure 2d), the separated shear layer intermittently rolls into the gap, intermittently reattaches to P2, or intermittently remains detached beyond P2; regime E1 (figures 2e and f) is similar but only the first two of these processes occur. In practice, it is difficult to distinguish between these two regimes on an array with $C_2 = 1$ at higher Reynolds numbers. In figure 2e the top separated shear layer rolls into the gap forming a vortex impinging on the leading edge corner of P2 while the bottom shear layer forms a vortex impinging on a streamwise surface of P2. As in regime F3 an occasional symmetric shedding, lasting few shedding cycles, can occur as shown in figure 2f. As Reynolds number is increased, small vortices which result from a secondary (Kelvin-Helmholtz) instability of the vortex sheet at a frequency much higher than that of the main vortex street, become evident on the separated shear layers but the general character of flow pattern does not change (figure 2g). Similar behaviour was observed in other flow regimes. When the gap becomes large, regime D is established (figure 2h), in which the separated shear layers penetrate the gap at all times and merge to form a von Karman vortex street within the gap. For an array with $C_1 = 1$, this type of flow is very little influenced by the value of C_2.

For the ($C_1 = 1$, $C_2 = 9$) array at small gaps, typically $G \leq 1$, the flow regime becomes F1 with reattachment on plate P2 at all times (figure 3a). There is no flow through the gap, flow within the gap consists of a pair of counter-rotating vortices, and the array behaves as a single plate. As Reynolds number is increased the separation bubble becomes shorter and laminar-turbulent transition occurs upstream of the reattachment. At higher Reynolds numbers at $G > 1$, the flow regime becomes E1 (figure 3b), with flow in the gap and secondary vortex formation. At still larger gaps, $G >\sim 3$, regime D becomes established, with a von Karman vortex street within the gap (figure 3c).

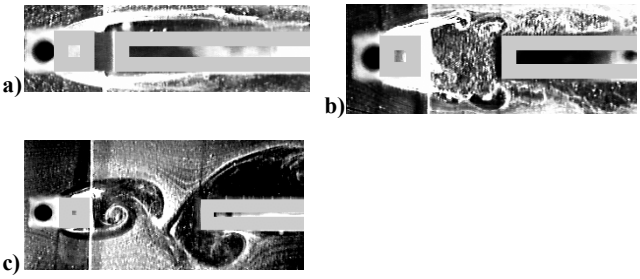

Figure 3. Flow over ($C_1 = 1$, $C_2 = 9$) array: (a) $G = 0.5$ at $Re_t \approx 600$, (b) $G = 2$ at $Re_t \approx 1300$ and (c) $G = 3.7$ at $Re_t \approx 600$.

Data for pressure coefficients and Strouhal numbers at $Re_t = 16 \times 10^3$ for the ($C_1 = 1$, $C_2 = 1$) array (presented in [1]) and the ($C_1 = 1$, $C_2 \approx 6$) array (figure 4) indicate different forms of variation associated with different flow regimes. In particular, large jumps in both surface pressures and Strouhal numbers occur when flow switches from regime E1 into regime D (flow with a von Karman street in the gap). This corresponds to a dramatic increase in the level of acoustic radiation. There is an overlap region for $2 < G < 3$ when flow can switch between regimes E1 and D. For the ($C_1 = 1$, $C_2 \approx 6$) array in regime E1, vortex shedding from the trailing edges of P2 has a frequency higher than that of the flow fluctuations in the gap. This shedding was not detected in acoustic radiation where the dominant spectral peaks occur at frequencies of characteristic flow fluctuations in the gap. In all other cases the characteristic frequencies measured in the gap and downstream of P2 coincide.

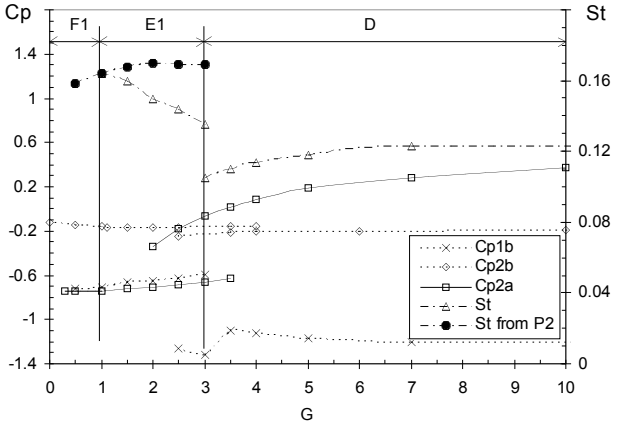

Figure 4. Dependence of Strouhal number and pressure coefficients on gap at $Re_t = 16 \times 10^3$ for ($C_1 = 1$, $C_2 \approx 6$) array. C_{p2a}: pressure coefficient on the front face of the downstream plate; C_{p1b}, C_{p2b}: base-pressure coefficients of both plates.

GROUP 2: plate configurations with $S_{min} < C_1 < S_{max}$

In this group of plates the possible flow regimes are B, C1 and C2. However in the flow visualisation around the plate configurations with short downstream plate, regime C2 was not observed. Instead, regime C1 was established as soon as G was greater than 0. The similarity between the variation of pressure coefficients and Strouhal number with G, for very small G, for the (C_1 = 3.56, C_2 = 1) and the (C_1 = 3.56, $C_2 \approx 6$) arrays also indicates that both arrays exhibit the same flow regimes. The only dramatic changes in the variation of pressure coefficients and Strouhal numbers, accompanied by dramatic increase in the level of acoustic radiation, occur at $G \approx 3.5$ for both plate configurations. It was therefore concluded that both arrays exhibit flow regimes C1 and B with the transition between them occurring at $G \approx 3.5$.

Figure 5a shows flow at G = 0.5 (regime C1) with the top separated shear layer reattaching on P2 (hydrogen bubbles generated by the wire located in the gap are entrained upstream) and with the bottom separated shear layer reattaching on P1 (hydrogen bubbles are swept downstream). In figure 5b (G = 3.7) the separated shear layers reattach intermittently on P1 and roll into the gap where they merge to form von Karman vortex street (regime B).

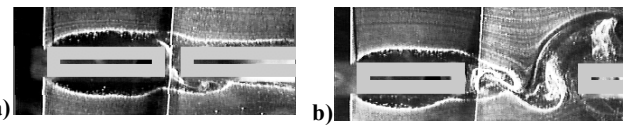

Figure 5. Flow over (C_1 =3.6, C_2 = 9) array at $Re_t \approx 600$: (a) G = 0.5 and (b) G = 3.7.

As for the (C_1 = 1, C_2 = 6) array in regime E1, in the (C_1 = 3.56, C_2 = 6) array at small gaps corresponding to regime C1, vortex shedding from the trailing edges of P2 has a frequency different to that of the flow fluctuations in the gap. This shedding was not detected in the acoustic radiation. In all other cases the characteristic frequencies measured in the gap and downstream of P2 coincide.

In acoustic spectra the dominant peaks at fundamental frequencies associated with flow regimes C1 and B, f_{C1a} and f_{Ba} respectively, agree well with the characteristic velocity fluctuation frequencies f_{C1v} and f_{Bv}, measured in the gap between plates. This indicates that the acoustic radiation results predominantly from vortex formation in the separated shear layer and their interaction with the plates. However, some of the acoustic spectra also exhibit a number of distinct low-frequency peaks which appear consistently over the range of investigated gaps. In regime C1 at larger gaps (G = 2, figure 6a) the low-frequency peaks at ~$1/3f_{C1a}$ and ~$1/2f_{C1a}$ appear consistently together with peak at f_{C1a}. The relative magnitudes of these peaks change with Reynolds number as the radiation is strongly influenced by the acoustic resonances, with the $1/3f_{C1a}$ peak becoming the dominating component of the radiation at lower flow velocities. The low frequency peaks in regime C1, at ~$1/3f_{C1v}$ and ~$2/3f_{C1v}$, were also detected in the velocity-fluctuation measurements for the (C_1 = 3.56, C_2 = 6.16) array at G = 3 with a hot-wire probe located in the gap (figure 6b) and also in surface pressure spectra. The acoustic spectra for regime B, shown in figure 6c for the configurations with G = 5, have distinct peaks at ~$1/3f_{Ba}$, ~$2/3f_{Ba}$ and f_{Ba}. Once the flow changes from regime C1 into regime B, with a regular von Karman vortex street in the gap, the low frequency component $1/3f_{Ba}$ becomes dominant through the entire investigated velocity range with an increase in acoustic radiation by about 10 dB (figure 6b for G = 5). In some cases a peak at frequency ~$5/3f_{Ba}$ was observed, indicating a non-linear interaction of the low-frequency components with fundamental frequencies. For a particular G the relative magnitudes of peaks do not change significantly within the investigated range of velocity, however the $2/3f_{Ba}$ peak becomes weaker as G is increased. The low-frequency peak at $1/3f_{Bv}$ was also detected in the flow-fluctuation spectra.

The low-frequency peaks are consistent with the frequencies detected in the current investigation in the flow around mid-length-chord single rectangular plates and the frequencies reported by Knisely and Rockwell [4] for the pressure and velocity fluctuations of a separated shear layer impinging on a corner. It is believed that these low-frequency components and their non-linear interaction with fundamental frequencies are associated with the variation in impingement location of successive vortices on the trailing-edge plate corners, arising from the amplified instability wave involving cycling between different classes of vortex-corner interaction as reported by Rockwell and Knisely [5]. However, unlike the case of single plates, the low frequency components can become the dominant source of acoustic radiation in the presence of the downstream plate.

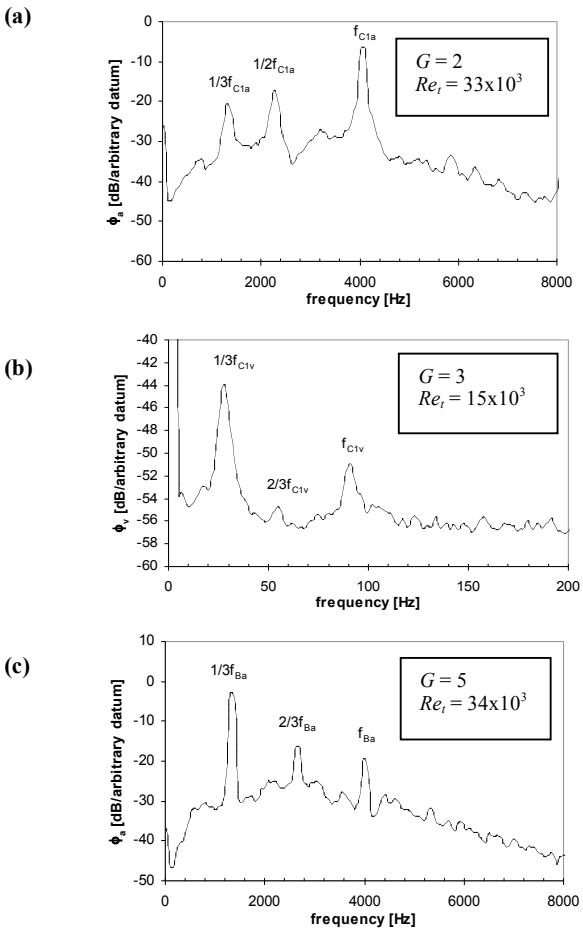

Figure 6. Frequency spectra for: (a) the (C_1 = 3.56, C_2 = 6.52, G = 2) array, Re_t = 33 x 10^3 (acoustic), (b) the (C_1 = 3.56, C_2 = 6.16, G = 3) array, Re_t = 15 x 10^3 (flow) and (c) the (C_1 = 3.56, C_2 = 6.52, G = 5), Re_t = 34 x 10^3 (acoustic).

GROUP 3: plate configurations with $C_1 > S_{max}$

In this group of plates, with a separation bubble formed permanently on the upstream plate and the gap between plates located downstream of the reattachment, the only possible flow regime is A (figure 1). This regime can be further subdivided into regimes A-1 and A-2, depending on the interaction between shear layers separated from the trailing edge of P1 and the leading edge of P2. In both cases the shear layers separated from

both sides of the trailing edge of P1 can either impinge on P2 without merging with each other (regime A-1) or they can form a regular von Karman vortex street (regime A-2).

For very small gaps the shear layers separating from the end of P1 reattach on P2 without penetrating across the gap (regime A-1), and the fluid trapped in the gap forms two counter-rotating vortices. These vortices can be symmetric, appearing for brief periods of few shedding cycles (figure 7a), but they are predominantly asymmetric (figure 7b). In general these patterns are similar to those observed in the flow around arrays having an upstream plate with an elliptic leading edge. However there are some differences due to the different character of the separated shear layers outside the gap. For the rectangular plates in tandem the shear layer separating from the leading edge of P1 undergoes laminar-turbulent transition before reattaching on the plate's surface, leading to a turbulent boundary layer on P1 with mixing-layer-like turbulence characteristics (see Castro and Epic [3]). This leads to a higher exchange rate of fluid between the shear layer, containing large-scale vortical structures, and the flow trapped in the gap. This exchange is accompanied by generally unstable and irregular flow in the gap.

For sufficiently large gaps the separated shear layers roll up to form vortices which impinge on the corners of the leading edge of P2 (figures 7c and 7d, $G = 2.0$). For this gap value the flow is bistable, switching intermittently between regimes A-1 and A-2. In regime A-1 of this case the shear layers bridging the gap do not merge; instead they form two separate vortex streets with almost stationary fluid trapped in the gap (figure 7c). In regime A-2 of this case, the separated shear layers merge immediately after separation from P1 and form a von Karman vortex street which impinges on leading edge of P2 (figure 7d).

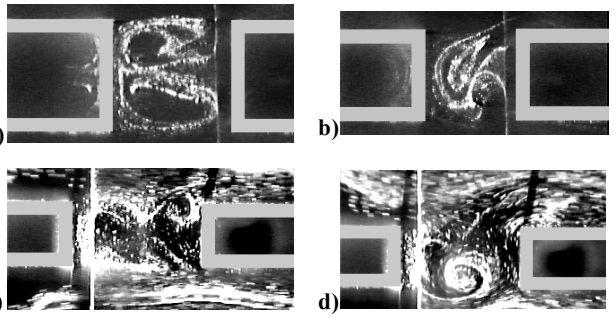

Figure 7. Flow over (C_1 =9, C_2 = 4) array at $Re_t \approx 600$: (a) G = 1, symmetric mode, (b) G = 1, asymmetric mode, (c) G = 2, non-merging vortex street, and (d) G = 2, von Karman vortex street..

Data for pressure coefficients and flow and acoustic Strouhal numbers were measured for the (C_1 = 23.31, C_2 = 1) and the (C_1 = 23.31, $C_2 \approx 6$) arrays. For both investigated arrays significant changes in the variation of pressure coefficients and Strouhal numbers associated with the transition between A-1 and A-2 flow regimes occur at $G \approx 2.5$. This transition is also accompanied by a dramatic increase in the level of acoustic radiation. For the gap range $2 < G < 3$ there is an overlap region in which either regime can exist.

In regime A-2, vortex shedding from the trailing edges of P2 has a frequency different to that of the flow fluctuations in the gap for any G for the (C_1 = 23.31, $C_2 \approx 6$) array, and at sufficiently large gaps ($G \geq 6$) for the (C_1 = 23.31, C_2 = 1) array. In regime A-1 the characteristic frequencies measured in the gap and downstream of P2 are the same.

The similarity of character and Strouhal number values of the peaks at fundamental shedding frequencies in the velocity and acoustic spectra for the ($C_1 \approx 23$, $C_2 \approx 6$ arrays) indicates that the acoustic radiation is predominantly caused by vortex formation in the separated shear layer and the interaction of those vortices with the plates. In the flow around configurations where vortex shedding from the trailing edges of P2 can have a frequency different to that of the flow fluctuations in the gap, acoustic radiation at the trailing edge shedding frequency was not detected.

Conclusions

The theoretically predicted flow regimes over two plates of rectangular cross-section were investigated and identified by flow visualisation, characteristic forms of variations of surface pressures, flow fluctuation frequencies and the level of acoustic radiation versus gap for selected plate arrays. Regime A was further subdivided into Regimes A-1 and A-2, depending on the interaction between shear layers separated from the trailing edge of P1 and the leading edge of P2. Comparisons between the predicted and measured regimes in terms of G ranges are given in table 1. The comparison gives an expected range of the general separation bubble lengths S_{min} and S_{max}. The only regime predicted theoretically and not observed in the current investigation is regime C2.

Reg.	Predicted G	Measured G
GROUP 1; $C_1 < S_{min}$; ($C_1 = 1$, $C_2 = 1$) array		
F3	$0 < G < [S_{min} - (C_1 + C_2)]$	$0 < G < 0.3$
F2	$0 < G < [S_{min} - C_1]$	$0.3 < G < 0.6$
E2	$[S_{min} - C_1] < G < [S_{max} - (C_1 + C_2)]$	$0.6 < G < 1.5$
E1	$[S_{max} - (C_1 + C_2)] < G < [S_{max} - C_1]$	$1.5 < G < 2.5$
D	$G > [S_{max} - C_1]$	$G > 2.5$
GROUP 1; $C_1 < S_{min}$; ($C_1 = 1$, $C_2 > 6$) array		
F1	$0 < G < [S_{min} - C_1]$	$0 < G < 1.0$
E1	$[S_{min} - C_1] < G < [S_{max} - C_1]$	$1.0 < G < 3.0$
D	$G > [S_{max} - C_1]$	$G > 3.0$
GROUP 2; $S_{min} < C_1 < S_{max}$; ($C_1 = 3.56$, $C_2 = 1$) and ($C_1 = 3.56$, $C_2 > 6$) arrays		
C1	$0 < G < [S_{max} - C_1]$	$0 < G < 3.5$
B	$G > [S_{max} - C_1]$	$G > 3.5$
GROUP 3; $C_1 > S_{max}$; ($C_1 = 23.31$, $C_2 = 1$) and ($C_1 = 23.31$, $C_2 \approx 6$) arrays		
A-1	-	$0 < G < 3$
A-2	-	$G > 2$

Table 1. Identified high-Reynolds-number flow regimes.

In all the acoustic measurements the dominant spectral peaks occur at the frequencies of characteristic flow fluctuations in the gap between plates, with the level of acoustic radiation strongly dependent on the flow regime established. The most dramatic increase in the level of radiation occurs during the transition to regimes with a regular, von Karman vortex-street in the gap (regimes A-2, B and D). This increase is accompanied by large changes of surface pressures on both plates.

In all the investigated cases, when vortex shedding from the downstream plate was detected in the flow at a frequency different to that of the flow fluctuations in the gap, this shedding was not detected in the acoustic radiation.

In regime C1 the acoustic radiation is dominated by the component at the fundamental frequency f_{C1a} at higher flow velocities and by the $1/3f_{C1a}$ component at lower velocities. Once the flow changes from regime C1 into regime B, with a von Karman vortex street in the gap, the low frequency component $1/3f_{Ba}$ becomes dominant through the entire investigated velocity range with an increase in acoustic radiation by about 10 dB.

A general conclusion of this work is that, in order to suppress aerodynamic noise, the gap-to-thickness ratio G between the plates should be less than about two, with the exact value of G depending on the specific tandem configuration and (weakly) the Reynolds number.

References

[1] Blazewicz A.M. and. Bull M.K., Acoustic radiation due to flow over tandem two-plate arrays. *Proc. 10th Int. Congress on Sound and Vibration,* 2003. 4499-4506.

[2] Bull M.K., Blazewicz A.M. and Pickles J.M., Acoustic radiation from a tandem two-plate array in a fluid flow: dependence on array geometry and flow regime. *Proc. 5th Int. Congress on Sound and Vibration,* 1997.

[3] Castro I.P. and Epik E., Boundary layer development after a separated region. *J. Fluid Mech.,* **374**, 1998, 91-116.

[4] Knisely C. and Rockwell D., Self-sustained low-frequency components in an impinging shear layer. *J. Fluid Mech*., **116**, 1982, 157-186.

[5] Rockwell D.O. and Knisely C., Vortex-edge interaction: Mechanics for generating low frequency components. *Phys. Fluids*, **23(2)**, 1980, 239-240.